RETRIEVAL OF SOIL MOISTURE USING ELECTROMAGNETIC MODELS AND A BAYESIAN APPROACH IN VIEW OF THE SAOCOM MISSION: STUDY ON SARAT IMAGES IN AN AGRICULTURAL SITE IN ARGENTINA

Romina Solorza[1], *Claudia Notarnicola*[2], *Haydee Karszenbaum*[3]

[1]Instituto Gulich, CONAE, Ruta C45, Km 8, 5187, Falda del Carmen, Córdoba, Argentina.
[2]EURAC, Institute for Applied Remote Sensing, Viale Druso 1, 39100 Bolzano.
[3]IAFE, Instituto de Astronomía y Física del Espacio. CONICET/UBA. Buenos Aires, Argentina.

ABSTRACT

The aim of this research is to examine the ability of an approach based on Bayesian inference to retrieve surface soil moisture in an experimental agricultural area located in the province of Córdoba, Argentina. Radar images from SARAT sensor were used, as well as measurements of biophysical parameters in the field. Several implementations of the main algorithm were designed to evaluate their different capability to reproduce the ground data. The Bayesian inversion was performed based on electromagnetic model: the Integral Equation Model (IEM) for bare soil, and the Water Cloud Model (WCM) for vegetated fields. For bare soil, the results showed high sensitivity of the algorithms to the different roughness conditions of each plot, while for vegetated areas, the availability of field measurements limited the comparisons between the obtained maps and the in situ data.

Index Terms— Soil Moisture, SAR, SARAT, Electromagnetic Models, Bayesian approach.

1. INTRODUCTION

Soil Moisture has an important role in the energy balance between the Earth's surface and the atmosphere, and hence, its relevance for different ecological processes. This environmental variable is being deeply studied in Argentina because of the near future launching of the first satellite of the SAOCOM mission (http://www.conae.gov.ar/satelites/saocom). In fact, there is a particular demand of soil moisture maps from agricultural farmers of the Pampa region for monitoring the crop status, possible evaluation of water demand and yield assessment. The estimation of soil moisture from SAR sensors is very complex, because many factors can contribute to the signal sensor response. The backscattering signal depends greatly on the moisture content, directly related to the dielectric constant of the soil (ε) and other factors such as soil texture, surface roughness and vegetation cover, being the latter the factors that may hinder a correct estimation of soil moisture [1]. The objective of this research is to examine the capability and accuracy of a Bayesian approach to retrieve surface soil moisture setting different roughness and vegetation conditions in view of an operational use of the algorithm . Several implementations of the main algorithm were designed to evaluate their different capabilities to reproduce the ground data. In most cases, these approaches are based on the assumption of predefined behavior of some parameters, such as vegetation and roughness, measured in situ, and then used as conditional probabilities. The Bayesian approach has the capability of adding this information and testing the calibration of the probability density function (PDF), minimizing the expected error [2, 3, 4]. The procedure adopted here was applied to data from SARAT L Band active sensor. The SARAT SAR is an airborne sensor used to simulate the SAOCOM images to be analyzed in feasibility studies. This study is the result of the thesis carried out in the framework of the Master in Emergency Early Warning and Response Space Applications (AEARTE), managed by Institute Gulich of the Argentinean Space Agency (CONAE) and Italian Space Agency (ASI) in the framework of the SIASGE project.

2. DATA SETS

The data set consists of field soil moisture content measurements with the corresponding backscattering coefficients at HH, HV, VH and VV polarizations and 25^o incidence angle acquired with a L-band SARAT sensor. SARAT project is a remote sensing experiment that is carried out in an agricultural area, located in Cordoba province, Argentina (http://www.conae.gov.ar/satelites/saocom/sarat.html). The experimental site, chosen for soil moisture, vegetation and surface roughness measurements, has 10 fields which contain soybean, sunflower, corn and wheat crops, and bare soil fields. Its central geographic coordinates are 31^o31'15.08"S - 64^o27'16.32"W. All fields were intensively sampled during the SARAT acquisitions. Figure 1 shows the distribution and denomination of the agricultural plots in the study area. All the data was provided by CONAE. The bare soil plots were ploughed with two roughness levels (low and high roughness) to evaluate the roughness impact on soil moisture retrieval

at plot level. Soil moisture varied between 4% and 40%, even though most plots showed medium-dry conditions. The SARAT images (resolution: 9 m ground range) were acquired on February 2012.

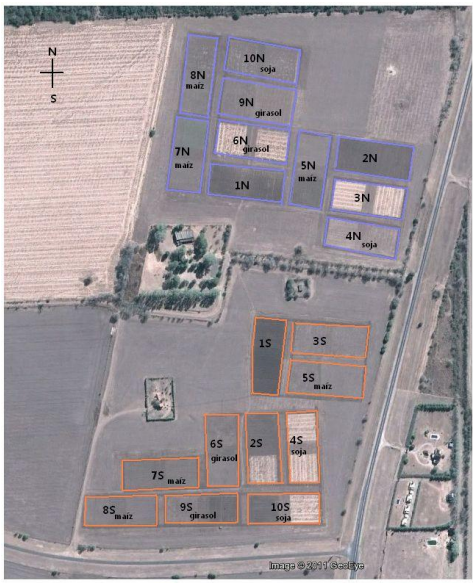

Fig. 1. Study area. Agricultural plots (SAOCOM mission experimental site) at CONAE, in Córdoba, Argentina. The 'N' plots are the northern ones and the 'S' plots are the southern. Plots without description are the ones without vegetation.

3. BAYESIAN SOIL MOISTURE APPROACH

In the Bayesian approach, the scope is to infer biophysical parameters (e.g. soil moisture), from a set of backscattering responses measured by the sensor. The algorithm is based on experimental data and theoretical models. The problem to have a large amount of experimental data to build a reliable PDF has been overcome by the use of the simulated data from theoretical models. The Integral Equation Model (IEM) [5] was selected because it has the advantage of being applicable to a wide range of roughness scales. The general condition of validity of the model is $ks < 3$, where k is the wave number ($cm^{-1} \approx 0.2732$ for 1.3 GHz). For bare soil, these unknown parameters are the real part of the dielectric constant (ε), the standard deviation of the height (s) and the correlation length (l), the latter two describing the morphology of the surface. For vegetated fields, the Bayesian inversion was performed based on the Water Cloud Model (WCM) [6], where the Vegetation Water Content (VWC) is added as unknown parameter. Calibration constant values of the WCM were taken from literature to take into account the effect of vegetation on the SAR signal.[7]. The application of calibration equations consider two different kind of vegetation, with respect to the sensor response: very dense vegetation (as corn and sunflower) and less dense vegetation (soybean and wheat). This step includes the NDVI calculation from some SPOT optical images acquired close in time to the SAR image. At the beginning, the conditional probability it is assumed as normal. In the training phase, the conditional PDF is evaluated using measured data (f_{im}) and simulated values from the IEM model (f_{th}). It is verified with a chi-squared statistics. The noise function N_l (eq. 1) and the PDF parameters (mean and standard deviation) are calculated.

$$N_i = \frac{f_{im}}{f_{ith}}, \tag{1}$$

The final PDF is a posterior probability derived from prior probability on roughness and soil moisture values and to the conditional probability which relates the variations of backscattering coefficients to variations of soil moisture and roughness. The relationship can be expressed as follows:

$$P(\varepsilon, s, l|\sigma^o_{HH}, \sigma^o_{VV}) = \frac{P_{pr}(\varepsilon, s, l) P_{post}(\sigma^o_{HH}, \sigma^o_{VV}|\varepsilon, s, l)}{P(\sigma^o_{HH}, \sigma^o_{VV})}, \tag{2}$$

Where $P_{pr}(\varepsilon, s, l)$ is the prior joint PDF, in which one includes all the prior information about the variables ε, s, l; $P_{post}(\sigma^o_{HH}, \sigma^o_{VV}|\varepsilon, s, l)$ is to be computed based on the observed values of $\sigma^o_{HH}, \sigma^o_{VV}$; $P(\sigma^o_{HH}, \sigma^o_{VV})$ is a normalization factor with an integration over all variables ε, s, l. Based on the field data, the integration ranges for Bayesian inference were selected as follows: roughness (s) from 0.5 to 1.8 cm, correlation length (l) from 5 to 20 cm, and dielectric values (ε) from 2 to 20 for a sandy loam soil type. Through these integrations, it is possible to associate to each pixel a value of dielectric constant, starting from the corresponding backscattering coefficient values. Finally, with the formula proposed by [8] the dielectric constant has been transformed to estimated values of soil moisture. The flowchart in Fig. 2 outlines the main steps of the algorithm, including training and test phase (or belief phase).

4. TEST OF THE ALGORITHM UNDER DIFFERENT ROUGHNESS PRIOR CONDITIONS

For Bayesian approach two main algorithms have been implemented, one to be used in case of bare or scarcely vegetated soils, the second one is devoted to the retrieval of soil moisture for vegetated soils. In both cases, an extended analysis has been carried out in order to understand the effect of other variables (such as roughness and vegetation) on the retrieval of soil moisture. For the bare soil algorithm, the Bayesian approach as already described in the general description of the retrieval procedure is based on the comparison between measured backscattering coefficients and simulated ones derived from IEM model. One point to be discussed is the information on the prior PDF for roughness. The following roughness conditions have been tested:

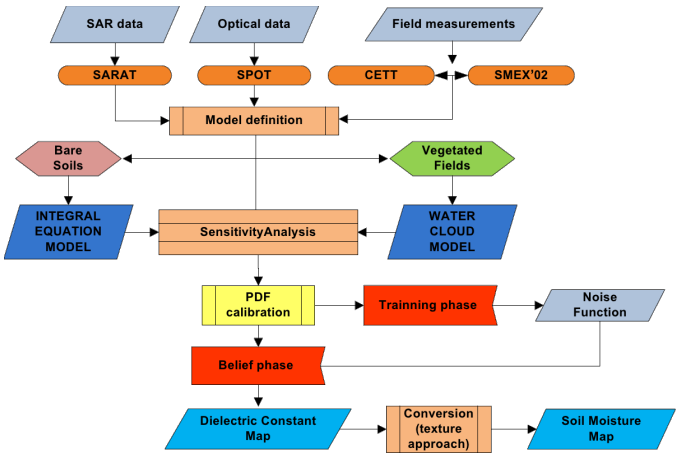

Fig. 2. Flowchart of the Bayesian soil moisture approach.

- Case 1: Pixel based algorithm for bare soil with fixed roughness. Three runs were executed: $s = 0.3$cm, $l = 5$cm; $s = 0.5$cm, $l = 5$cm and $s = 0.9$cm, $l = 5$cm. Then a mean value map is generated.
- Case 2: Pixel based algorithm for bare soil with an integration over a roughness range. $0.6\text{cm} < s < 1.4\text{cm}$; $l = 5$cm.
- Case 3: Pixel based algorithm for bare soil with an integration over a roughness range. $0.6\text{cm} < s < 1.4\text{cm}$; $l = 15$cm.
- Case 4: Pixel based algorithm for bare soil with an integration over a roughness range. $1\text{cm} < s < 1.5\text{cm}$; $l = 5$cm. In this case a very small integration range was considered.
- Case 5: Algorithm applied to backscattering coefficients averaged at plot level with a random function. Values range: $0.5\text{cm} < s < 1.2\text{cm}$; $5\text{cm} < l < 10\text{cm}$.
- Case 6: VWC is calculated using a SPOT image. Fixed roughness and correlation length. $s = 0.5$cm; $l = 5$cm.
- Case 7: VWC is calculated using a SPOT image and a random function is implemented for s and l calculation, considering expected mean and standard deviation values for each parameter: Mean value of $s = 0.7$cm and standard deviation value of 0.5cm, mean value of $l = 5$cm and standard deviation of 5cm.
- Case 8: VWC is provided as an input variable and an integration is done over the following values: $0.01 < VWC < 6\ Kg/m^2$.
- Case 9: VWC is calculated using a SPOT image, based on NDVI values, and an integration is done over roughness and correlation length in the following ranges:$0.4\text{cm} < s < 1.2\text{cm}$ and $3\text{cm} < l < 10\text{cm}$.

5. RESULTS AND CONCLUSIONS

In order to optimize the accuracy of the results and to verify the sensitivity of the algorithm to prior conditions of roughness and vegetation, several retrievals were performed for different conditions of surface roughness, with specific algorithms for each coverage type in the study area. Two main algorithms were implemented: one to be used where bare soil or covered with sparse vegetation and another for vegetated soils. In both cases, two versions of the algorithm were developed: a simplified one working on a vector of mean values for each plot where the aim is to analyze the backscatter coefficient behavior using random values within ranges of s and l, and another one working at a pixel level to investigate the spatial pattern of soil moisture. In both cases, an extensive analysis was conducted in order to understand the behavior of variables such as surface roughness and vegetation presence in the final soil moisture estimation. In Fig. 3, preliminary results are presented where the different analyzed cases based on various prior conditions are numbered from 1 to 9. In general, for bare soil, the results showed a sensitivity of the algorithms to the different roughness conditions of each plot with a variability of around 5-7% (excluding the extreme cases), while for vegetated areas, due to the limited availability of field measurements the evaluation of the performances is still under work.

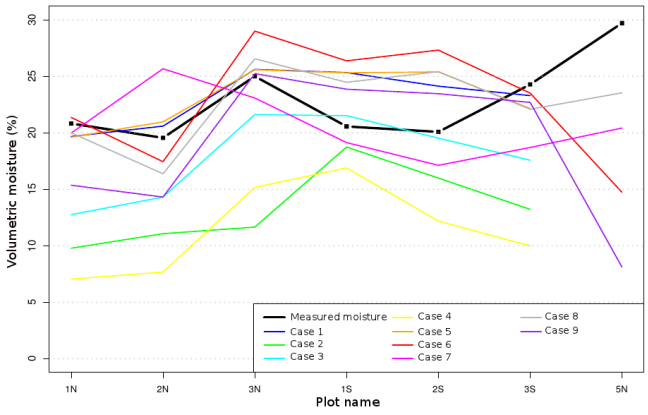

Fig. 3. Behavior diagram of the described cases. Comparison with measured data.

From the analysis at field level, error patterns are detected for cases with rows of plots oriented orthogonally to the direction of the sensor observation. As it was observed that the response HH is sensitive to the orientation of lines tillage and no inversion algorithms consider this factor, the results show significant errors in plots perpendicular to the observation.

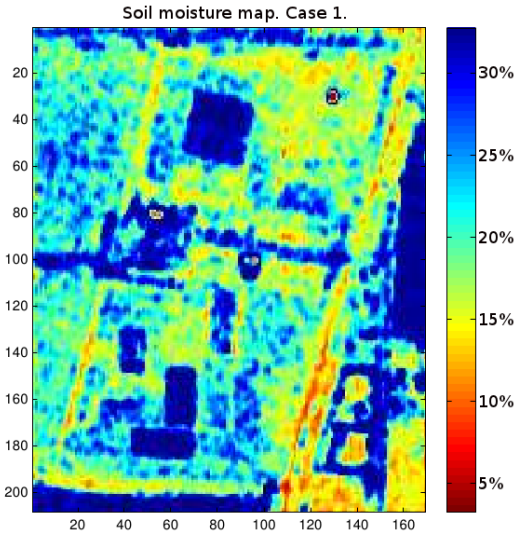

Fig. 4. Soil moisture map for Case 1 over the selected test site.

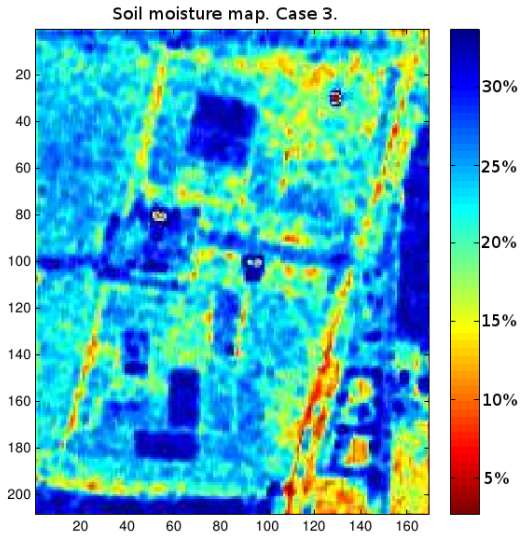

Fig. 5. Soil moisture map for Case 3 over the selected test site.

Case 1 shows that the northern plots with bare soils (1N and 2N) have moisture values very similar to the ground truth. On the contrary, southern plots with bare soils (1S and 2S) have higher moisture values than the measured ones, having the first of them a value of 25%, while the in situ data shown values around 20%. Case 3 shows that plots 1N and 2N obtained moisture values around 15%, which represents an under-estimation of the actual value of around 5%. For plots 1S and 2S, the estimate is better, obtaining values between 22 to 24%. Case 1 could model with good accuracy plots 1N and 2N losing accuracy in southern plots. On the contrary, Case 3 could model with relatively accuracy plots 1S and 2S losing accuracy in northern plots. The factor of apparent roughness change is given by the orientation of the ploughing rows with respect to the SAR signal.

6. ACKNOWLEDGEMENTS

The authors wish to thank to CONAE and SAOCOM mission team for SARAT data provision and field measurements acquired during the remote sensing campaign.

7. REFERENCES

[1] B. Barrett, E. Dwyer, and P. Whelan, "Soil moisture retrieval from active spaceborne microwave observations: An evaluation of current techniques," *Remote Sensing*, vol. 1, pp. 210–242, 2009.

[2] C. Notarnicola and F. Posa, "Bayesian algorithm for the estimation of the dielectric constant from active and passive remotely sensed data," *IEEE Geoscience and Remote Sensing Letters*, vol. 1, no. 3, pp. 179–183, 2004.

[3] M. Barber, F. Grings, P. Perna, C. Bruscantini, and H. Karszenbaum, "Análisis de las mediciones de rugosidad del Centro Espacial Teófilo Tabanera, Córdoba," Tech. Rep., CONAE - IAFE, May 2011.

[4] P. Pampaloni, E. Santi, S. Paloscia, S. Pettinato, and P. Poggi, "Radar Remote Sensing of Soil Moisture - ENVISNOW Project - SMC algorithms," Tech. Rep., IFAC - CNR, October 2004.

[5] A. Fung, Z. Li, and K. Chen, "Backscattering from a randomly rough dielectric surface," *IEEE TRANSACTIONS ON GEOSCIENCE AND REMOTE SENSING*, vol. 30, pp. 356–369, 1992.

[6] E. P. Attema and F.T. Ulaby, "Vegetation Modeled as a Water Cloud," *Radio Science*, vol. 13, no. 2, pp. 357–364, 1978.

[7] T. Jackson, D. Chen, M. Cosh, F. Li, M. Anderson, C. Walthall, P. Doriaswamy, and E. Ray Hunt, "Vegetation water content mapping using landsat data derived normalized difference water index for corn and soybeans.," *Remote Sensing of Environment*, vol. 92, pp. 475–482, 2004.

[8] M.T. Hallikainen, F.T. Ulaby, M.C. Dobson, M.A. El Rayes, and L.K. Wu, "Microwave dielectric behavior of wet soil-part 1: Empirical models and experimental observations," *IEEE TRANSACTIONS ON GEOSCIENCE AND REMOTE SENSING*, vol. GE-23, no. 1, pp. 25–34, 1985.